Inorganic Chemistry

Article

pubs.acs.org/IC

Single-Crystalline Organic–Inorganic Layered Cobalt Hydroxide Nanofibers: Facile Synthesis, Characterization, and Reversible Water-Induced Structural Conversion

Xiaodi Guo, Lianying Wang,* Shuang Yue, Dongyang Wang, Yanluo Lu, Yufei Song, and Jing He

State Key Laboratory of Chemical Resource Engineering, Beijing University of Chemical Technology, Box 98, 15 Beisanhuan Dong Lu, Beijing 100029, P. R. China

Supporting Information

ABSTRACT: New pink organic–inorganic layered cobalt hydroxide nanofibers intercalated with benzoate ions [$Co(OH)(C_6H_5COO)\cdot H_2O$] have been synthesized by using cobalt nitrate and sodium benzoate as reactants in water with no addition of organic solvent or surfactant. The high-purity nanofibers are single-crystalline in nature and very uniform in size with a diameter of about 100 nm and variable lengths over a wide range from 200 μm down to 2 μm by simply adjusting reactant concentrations. The as-synthesized products are well-characterized by scanning electron microscope (SEM), transmission electron microscopy (TEM), high-resolution transmission electron microscopy (HRTEM), fast Fourier transforms (FFT), X-ray diffraction (XRD), energy dispersive X-ray spectra (EDX), X-ray photoelectron spectra (XPS), elemental analysis (EA), Fourier transform infrared (FT-IR), thermogravimetric analysis (TGA), and UV–vis diffuse reflectance spectra (UV–vis). Our results demonstrate that the structure consists of octahedral cobalt layers and the benzoate anions, which are arranged in a bilayer due to the π–π stacking of small aromatics. The carboxylate groups of benzoate anions are coordinated to Co^{II} ions in a strong bridging mode, which is the driving force for the anisotropic growth of nanofibers. When NaOH is added during the synthesis, green irregular shaped platelets are obtained, in which the carboxylate groups of benzoate anions are coordinated to the Co^{II} ions in a unidentate fashion. Interestingly, the nanofibers exhibit a reversible transformation of the coordination geometry of the Co^{II} ions between octahedral and pseudotetrahedral with a concomitant color change between pink and blue, which involves the loss and reuptake of unusual weakly coordinated water molecules without destroying the structure. This work offers a facile, cost-effective, and green strategy to rationally design and synthesize functional nanomaterials for future applications in catalysis, magnetism, gas storage or separation, and sensing technology.

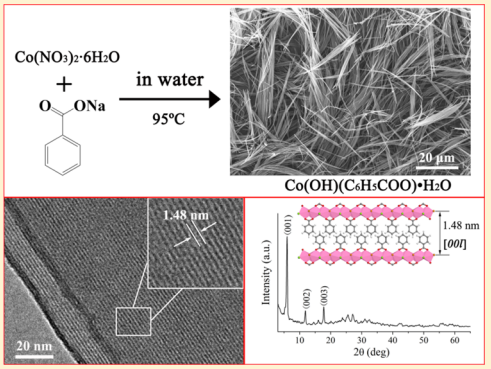

INTRODUCTION

Over the past decades, one-dimensional (1D) nanostructures (such as nanowires, nanotubes, nanobelts, and nanorods) have received significant research attention due to their intriguing properties and promising applications.[1−4] Recently, much attention has been paid to 1D organic–inorganic nanomaterials owing to their charming and unique properties. They are believed to combine the superior features of both inorganic frameworks and organic components, thus improving their functionality and performance. Meanwhile, some new physicochemical properties, e.g., tailored optical, electronic, and thermal properties, will be generated.[5] Additionally, the 1D organic–inorganic nanomaterials are also important precursors to achieve novel metal oxide, sulfide, nitride, and carbide nanostructures via secondary treatments, indicating new opportunities to design various functional materials.[6] Designing new 1D organic–inorganic nanomaterials will certainly open up exciting opportunities for developing a new class of electronically, optically, and biologically active materials.

Layered metal hydroxide compounds with a brucite-like structure can be classified into two types. One is layered double hydroxides (LDHs) with a general formula of $[M^{2+}_{1-x}M^{3+}_{x}(OH)_2]A^{n-}_{x/n}\cdot mH_2O$, where M^{2+} and M^{3+} are different kinds of divalent and trivalent metal ions, respectively, in the octahedral site of brucite-type hydroxide layers and A^{n-} is an interlayered anion to keep a whole charge balance.[7] The other is layered hydroxide metal salts (LHSs) with a general formula $[M^{2+}(OH)_{2-x}]A^{n-}_{x/n}\cdot mH_2O$, in which M^{2+} is the metal cation (e.g., Ni^{2+}, Co^{2+}, Cu^{2+}, and Zn^{2+}) and A^{n-} is the counter anion (e.g., Cl^-, NO^{3-}, SO_4^{2-}, and $CHCOO^-$).[8] Among the LHSs, layered cobalt hydroxides intercalated with various organic anions have attracted great interest due to the prominent properties and applications in magnetism, catalysis, and optoelectronics.[9,10] To date, a variety of procedures, such as solvent precipitation, microwave-assisted routes, anion exchange, and hydrothermal/solvothermal approaches, have been employed in attempts to

Received: July 28, 2014
Published: November 26, 2014

 © 2014 American Chemical Society dx.doi.org/10.1021/ic501812n | Inorg. Chem. 2014, 53, 12841−12847

prepare organic−inorganic layered cobalt hydroxides, such as $Co(OH)_{1.67}(DS)_{0.33}\cdot 1.1H_2O$ (DS = dodecyl sulfate), $Co_5(OH)_8(C_7H_{15}CO_2)_2\cdot 4H_2O$, $Co(OH)_{2.23}(CO_3)_{0.06}(AQS2)_{0.28}\cdot 0.68H_2O$ (AQS2 = anthraquinone-2-sulfonate), and so on.[9−11] However, most of these procedures typically involve organic solvents, surfactants, complex manipulations, and equipment, leading to high costs of the product and often yielding impurities. Moreover, most of the organic−inorganic layered cobalt hydroxides synthesized so far are poorly crystalline, in which the layers are randomly oriented about the *c*-axis, and the morphologies are irregular particles, plates, and other shapes; few studies have focused on the synthesis of organic−inorganic layered cobalt hydroxides nanofibers. Therefore, it still remains a great challenge to synthesize and characterize organic−inorganic layered cobalt hydroxide nanofibers in a facile and controlled fashion in order to rationally exploit their nanoscale physical and chemical properties, as well as to understand the factors that play a key role in their formation.

Here, we report the facile synthesis and characterization of high-quality, single-crystalline organic−inorganic layered cobalt hydroxide nanofibers. The synthetic route used here is very simple and involves directly mixing solutions of cobalt(II) ions and benzoate anions in water with no addition of organic solvent or surfactant or modulator, and requires no expensive or complicated equipment, while giving highly uniform nanofibers with 100 nm in diameter and controllable aspect ratios. To the best of our knowledge, this is the first report on the synthesis of single-crystalline organic−inorganic layered cobalt hydroxide nanofibers. Our study demonstrates that the formation of nanofibers is determined by the nature of the crystal structure, and a coordination-driven mechanism is proposed for the anisotropic growth of the hybrid nanofibers. More importantly, the resulting layered cobalt hydroxide nanofibers exhibit a novel reversible crystal-to-crystal transformation with a concomitant color change induced by dehydration at low temperature.

EXPERIMENTAL SECTION

Synthesis. All chemicals were analytical grade and used as received without further purification. In a typical procedure, an aqueous solution (100 mL) of $Co(NO_3)_2\cdot 6H_2O$ (0.02 mol) was added to an aqueous solution (150 mL) of C_6H_5COONa (0.04 mol) under continuous stirring at room temperature. The mixture was treated at 95 °C for 48 h. The resulting pink product was separated by centrifugation, washed repeatedly with distilled water, and directly dried in an oven at 40 °C in air.

Characterization. X-ray diffraction (XRD) patterns of the samples was recorded using a Shimadzu XRD-6000 diffractometer under the following conditions: 40 kV, 30 mA, Cu Kα1 radiation (λ = 0.154 06 nm). The samples were step-scanned in steps of 10°/min in the 2θ range from 3° to 70°. The observed diffraction peaks were corrected using elemental Si as an internal standard. Fourier transform infrared (FT-IR) spectra were recorded in the range 4000−400 cm^{-1} with 2 cm^{-1} resolution on a Bruker Vector-22 Fourier transform spectrometer using the KBr pellet technique (1 mg of sample in 100 mg of KBr). Thermogravimetric analysis (TGA) was carried out using a Rigaku TG-8120 instrument in the temperature range 25−800 °C at a heating rate of 10 °C/min under a nitrogen flow. Scanning electron microscope (SEM) images were obtained using a Hitachi S-4700 field emission SEM at 20 kV, with the surface of the samples coated with a thin platinum layer to avoid a charging effect. Transmission electron microscopy (TEM) was performed on a Hitachi H-800 microscope with an accelerating voltage of 150 kV. The sample was ultrasonically dispersed in an appropriate amount of water, and a drop of the resulting suspension was deposited on a carbon-coated Cu grid followed by evaporation of the solvent in air. HRTEM observations were carried out using a JEOL JEM-2010 electron microscope with an accelerating voltage of 200 kV. The sample was ultrasonically dispersed in an appropriate amount of water, and a drop of the resulting suspension was deposited on a carbon-coated Cu grid followed by evaporation of the solvent in air. The fast Fourier transform (FFT) images were obtained from selected areas of lattice images with the program Digital Micrograph (Gatan). X-ray photoelectron spectra (XPS) were recorded on a Thermo VG ESCALAB 250 X-ray photoelectron spectrometer at a pressure of about 2×10^{-9} Pa using Al Kα X-rays as the excitation source. Energy dispersive X-ray spectra (EDX) were recorded on energy dispersive X-ray detector. Elemental analysis (EA) was carried out using an Elementar vario MICRO cube instrument. UV−vis diffuse reflectance spectra were recorded at room temperature in air on a Shimadzu UV-2450 spectrophotometer.

RESULTS AND DISCUSSION

The morphology and particle size of the as-synthesized product were characterized by scanning electron microscopy (SEM). The low-magnification SEM image (Figure 1a) reveals that the

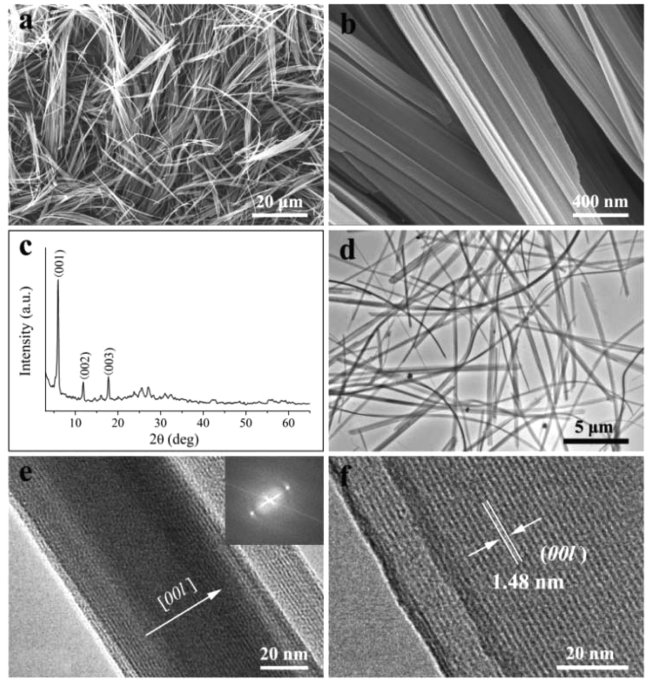

Figure 1. As-synthesized $Co(OH)(C_6H_5COO)\cdot H_2O$ nanofibers: (a) low- and (b) high-resolution SEM images; (c) PXRD pattern; (d) TEM image; (e, f) HRTEM images. The inset in panel e is the corresponding FFT pattern.

typical products consist of a large quantity (almost 100%) of nanofibers with lengths of about 20 μm. The SEM image at higher magnification (Figure 1b) clearly shows that the nanofibers are uniform along their length with an average diameter of about 100 nm and tend to be aligned in parallel to form bundles during sample preparation. The X-ray diffraction (XRD) pattern of the as-synthesized nanofibers (Figure 1c) shows the typical pattern of a layered structure with very well-ordered (00l) basal peaks at low angle. The peaks can be indexed as (001) (5.95°, 14.80 Å), (002) (11.85°, 7.46 Å), and (003) (17.78°, 4.98 Å). The narrow sharp peaks suggest that the product is highly crystalline. Considering the length of the

dx.doi.org/10.1021/ic501812n | Inorg. Chem. 2014, 53, 12841−12847

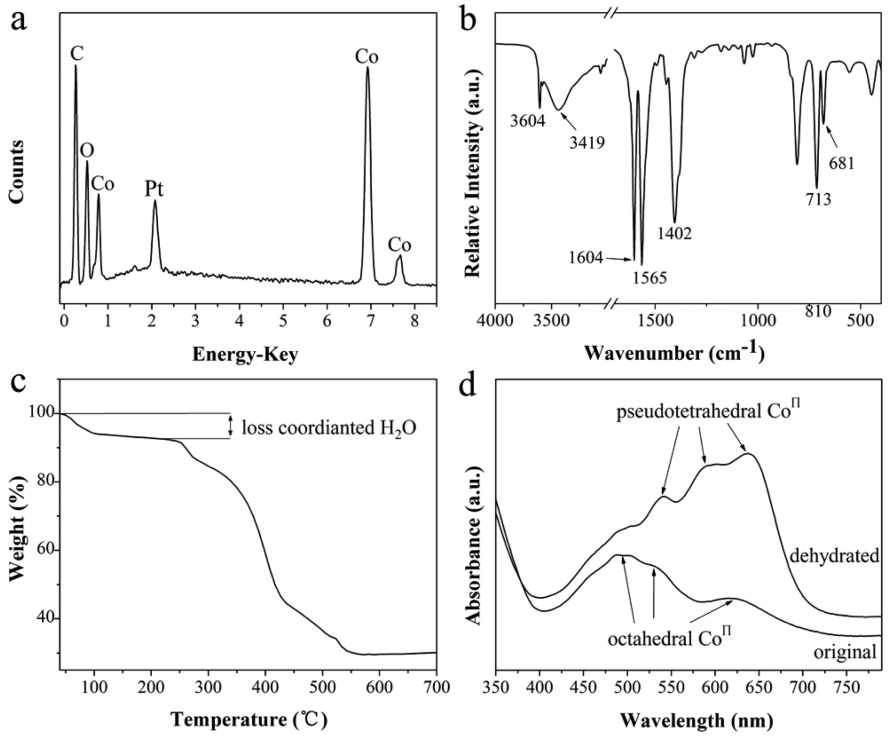

Figure 2. (a) EDX spectrum of $Co(OH)(C_6H_5COO)\cdot H_2O$ nanofibers, (b) FTIR spectra of $Co(OH)(C_6H_5COO)\cdot H_2O$ nanofibers, (c) TGA curve of $Co(OH)(C_6H_5COO)\cdot H_2O$ nanofibers, and (d) UV−vis spectra of $Co(OH)(C_6H_5COO)\cdot H_2O$ nanofibers before and after dehydration at room temperature under vacuum for 10 min.

benzoate anion (7 Å), the results suggest the formation of stacked double layers of benzoate anions.[12]

We further examined the microstructure of the product by transmission electron microscopy (TEM). Figure 1d shows a low-magnification TEM image of a typical sample cast from a colloidal suspension onto a substrate, confirming that the as-prepared sample is dominated by fiber-like nanostructures with high purity and morphological uniformity. It is known that organic−inorganic hybrid materials are unstable in an ultrahigh vacuum and often appear amorphous in TEM. In addition, the vast majority of organic−inorganic hybrid materials are extremely electron beam unstable.[13] Fortunately, the high-resolution TEM (HRTEM) images (Figure 1e,f) demonstrate that nanofibers have high beam-stability and clearly show a layered stacked structure with an interlayer *d*-spacing of 1.48 nm, which is consistent with the XRD data. The clear lattice fringes in Figure 1f show that the nanofibers are well-crystallized. The inset in Figure 1e is the corresponding fast Fourier transformation (FFT) pattern, which confirms the single-crystalline nature of the samples. Furthermore, from the HRTEM results and FFT pattern, it can be deduced that the growth orientation is perpendicular to the [00l] direction. The results also indicate a tendency for the nanofibers to orient with their (00l) planes perpendicular to the substrate, which may result from the hydrophobic nature of the (00l) planes capped with aromatic rings.

The EDX spectrum of the nanofibers (Figure 2a) shows the presence of Co, O, C (with additional Pt signals arising from the Pt coating). The ratio between Co ions and benzoate groups is estimated to be 1:1 with no detectable N content, confirming the absence of cointercalation of NO_3^- from the $Co(NO_3)_2$ precursor. The X-ray photoelectron spectrum (XPS) of the nanofibers shows three binding energy peaks at 781.2, 782.7, and 786.2 eV (Supporting Information Figure S1) confirming that the cobalt ions are divalent.[14] The EDX and XPS results are consistent with the chemical composition $Co(OH)(C_6H_5COO)\cdot H_2O$ suggested by the elemental analysis results. (Anal. Calcd: C 39.08, H 3.72%. Found: C 39.15, H 3.52%.) Although there have been reports of other cobalt benzoate compounds prepared in nonaqueous processes,[15] to the best of our knowledge, the synthesis of the $Co(OH)(C_6H_5COO)\cdot H_2O$ has never been reported.

Fourier transform infrared (FTIR) spectroscopy is a very useful tool in the characterization of layered metal hydroxides, especially those containing interlayer organic anions, as it is very sensitive to the interactions between the interlayer anions and the host layers. The FTIR spectrum of the nanofibers is illustrated in Figure 2b. The intense and sharp peak at 3604 cm^{-1} is attributed to the O−H stretching mode of non-hydrogen bonded Co−OH groups, and is characteristic of the brucite-like structure.[8b] The broad band centered 3419 cm^{-1} is attributed to the vibration of hydroxyl groups of water molecules. The aromatic ring of benzoate anions is evidenced by three bands at 1604 cm^{-1} (C═C stretching mode), 713 cm^{-1}, and 681 cm^{-1} (−C−H antiplane bending mode).[16] The strong bands centered at 1565 and 1402 cm^{-1} are assigned to the asymmetric ν_{as}(COO) and symmetric ν_s(COO) stretching modes of the carboxylate groups of the intercalated benzoate anions, and hence, the existence of benzoic acid molecules can be ruled out. The wavenumber difference $\Delta\nu = \nu_{as} - \nu_s$ gives information about the coordination environment of the carboxylate group. The value of $\Delta\nu$ is 163 cm^{-1} suggesting the carboxylate group is coordinated to the metal in a bridging bidentate fashion.[17] The absence of a band at about 1360 cm^{-1}, which would be expected for the υ_3 vibration mode of carbonate groups, excludes the possibility of contamination of

dx.doi.org/10.1021/ic501812n | *Inorg. Chem.* 2014, 53, 12841−12847

carbonate anions from the air and further confirms the high composition purity of the nanofibers.

The thermogravimetric analysis (TGA) trace for the $Co(OH)(C_6H_5COO)\cdot H_2O$ nanofibers performed under flowing N_2 is given in Figure 2c. The first stage between 40 and 100 °C shows a gradual weight loss of 8.21%, which corresponds to the loss of one water molecule per formula unit (calcd: 8.37%). There is no weight loss from 100 to 250 °C, and at higher temperatures the framework starts to decompose due to the dehydroxylation of the brucite-like layers accompanied by the decomposition of interlayer benzoate anions. Surprisingly, we found that the easily removable water molecule is coordinated to the Co^{II} ion, as demonstrated by a concomitant color change from pink to blue during the water loss process. Indeed, the coordinated water can be completely removed at room temperature under vacuum in no more than 10 min. The UV−vis spectrum (Figure 2d) of the original nanofibers reveals three absorption bands at 498, 530, and 614 nm that are characteristic of Co^{II} ions in an octahedral geometry. They are similar to the bands observed for β-$Co(OH)_2$ and correspond to the respective electron transitions $^4T_{1g}(F) \rightarrow {}^4T_{1g}(P)$, $^4T_{1g}(F) \rightarrow {}^4A_{2g}(P)$, and $^4T_{1g}(F) \rightarrow {}^4A_{2g}(F)$.[18] The change in color after dehydration, with absorption bands at 540, 590, and 638 nm, can be assigned to the $^4A_{2g}(F) \rightarrow {}^4T_1(P)$ transition (ν_3 band) of high-spin pseudotetrahedral Co^{II} ions.[19]

When the dehydrated nanofibers were exposed to air for several minutes or immersed in water at room temperature, they completely reverted to their initial color. The TGA trace of the rehydrated sample (Supporting Information Figure S2) is identical to that of the initial product showing that the nanofiber is able to reabsorb one water molecule and that the transformation is reversible. Figure 3 is a photograph giving a visual demonstration of the reversible color change behavior, which also demonstrated that the materials can be fabricated in large quantity via a cost-effective process. Importantly, the crystalline structure is kept intact after exposure to boiling water for 2 days (Supporting Information Figure S3), giving reproducible proof of their hydrothermal stability.

Figure 3. Photographs of $Co(OH)(C_6H_5COO)\cdot H_2O$ nanofibers in (a) hydrated and (b) dehydrated forms. The nanofibers exhibit a reversible transformation of the coordination geometry of the Co^{II} ions between octahedral and pseudotetrahedral induced by heating at low temperature, which involves the loss and reuptake of unusual weakly coordinated water molecules without loss of crystallinity.

These results demonstrate that the loss and reuptake of the coordinated water molecule interchanges the coordination geometry of the Co^{II} ions between octahedral and pseudotetrahedral. It is noteworthy that, during the processes of SEM, TEM, and HRTEM characterization, the nanofibers were dehydrated by evacuation within the electron microscope for several 10 min. Therefore, the electron microscopy results obtained here can be regarded as evidence for the maintenance of an intact morphology and layered structure after loss of the coordinated water, demonstrating that the transformation is crystal-to-crystal. This process is analogous to that observed for $Co(OH)(salicylate)\cdot H_2O$ except that the transformation in this material is initiated by the removal of the coordinated hydroxide group at much higher temperature (200−400 °C).[20] Such processes are known for some other coordination frameworks, and Kitagawa has termed these "type III" materials.[21] However, the coordination frameworks reported in the literature generally undergo reversible structural transformation upon removal of coordinated water by heating above 100 °C.[22] It is particularly noteworthy that the breaking of coordinate bonds in the layered cobalt hydroxide nanofibers takes place at such a low temperature, and supports the idea that they have great potential for utility in the world of materials chemistry.

While searching for the optimum conditions for the synthesis of organic−inorganic layered cobalt hydroxide nanofibers, we observed the formation of different materials when NaOH was added during the synthesis. For example, green irregular shaped platelets with a diameter of 100−200 nm and an average thickness of 30 nm were obtained if the pH of the reaction mixture was adjusted to 8 with 0.5 M NaOH solution (Figure 4). EDX and TGA studies (Supporting Information Figures S4 and S5) suggest that these nanoplates have the formula $Co(OH)_{1.7}(C_6H_5COO)_{0.3}\cdot 0.6H_2O$. The XRD pattern and UV−vis spectrum (Supporting Information Figures S6 and S7) together with its green color (see the inset in Figure 4) suggest that the structure of the nanoplates is similar to that reported for $Co(OH)_{1.70}Cl_{0.26}(CO_3)_{0.02}\cdot 0.56H_2O$,[23] $Co_5(OH)_8(C_7H_{15}COO)_2\cdot 4H_2O$,[9c] and $Co_5(OH)_8$(*trans*-1,4-cyclohexanedicarboxylate)$\cdot 4H_2O$.[9f] This structure consists of edge-sharing $Co^{II}O_6$ octahedra, with one-quarter of the octahedral sites vacant and two Co^{II} ions occupying tetrahedral sites located above and below the empty octahedral site. The anions coordinate in a unidentate fashion to the fourth corners of the tetrahedron in place of hydroxide ions. The FTIR spectrum of the green nanoplatelets shows carboxyl stretching frequencies at 1541 and 1395 cm^{-1} (Supporting Information Figure S8). The value of $\Delta\nu$ (146 cm^{-1}) for this unidentate coordination

Figure 4. SEM image of the organic−inorganic α-$Co(OH)_2$ nanoplates intercalated with benzoate anions obtained by precipitation with NaOH. The inset is a photograph of the material.

dx.doi.org/10.1021/ic501812n | *Inorg. Chem.* 2014, 53, 12841−12847

Scheme 1. Schematic Illustration of the Formation Process and Structure of $Co(OH)(C_6H_5COO)\cdot H_2O$ Nanofibers[a]

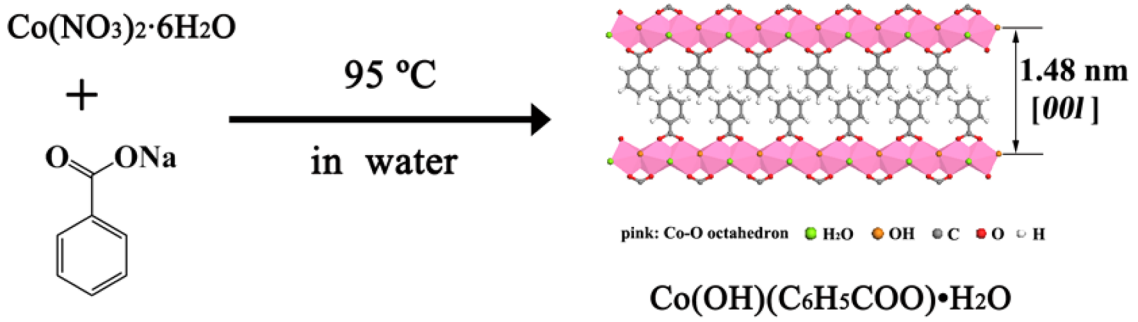

[a]The strong bridging coordination bonds between Co^{II} ions and interlayer benzoate anions is the driving force for the anisotropic growth of the 1D nanostructure.

mode in the green α-$Co(OH)_2$ is much smaller than 200 cm^{-1}, because the second oxygen atom of the carboxylate groups is involved in hydrogen bonds with the structural water molecules.[24] We also investigated the effect of the reaction temperature on the formation of $Co(OH)(C_6H_5COO)\cdot H_2O$ nanofibers and found that the reaction temperature was important for the formation of nanofibers. Under otherwise identical conditions as described in the Experimental Section, a larger number of nonuniform nanofibers with low crystallinity were obtained when the experiments were carried out at temperatures below 95 °C, and nothing was generated below 30 °C. The higher temperatures often result in the formation of impurity phases, in which nucleation and growth of metal oxide becomes possible.[25] For example, when the experiment was carried out at 180 °C, Co_3O_4 nanoparticles were obtained.

On the basis of the above results, the formation and structure of layered cobalt hydroxide nanofibers is illustrated in Scheme 1. The synthetic approach is very simple and involves directly mixing solutions of cobalt(II) ions and benzoate anions in water. The structure consists of octahedral brucite layers with vacant hydroxyl sites, and the benzoate anions are incorporated into the vacancies in the octahedral layers to directly coordinate to the Co^{II} ions. Because of the 50% substitution of hydroxyl groups, one benzoate anion must provide two oxygen atoms for coordination with Co^{II} ions within the layers. One Co^{II} ion is covalently bonded with two hydroxyl groups and two oxygen atoms belonging to benzoate anions to form unsaturated four-coordinate sites. The water molecules link relatively weakly to the Co^{II} ions giving coordinatively saturated octahedral centers. Therefore, the stronger bridging coordination bonds between Co^{II} ions and benzoate anions, which hold the structure together, are the driving force for the anisotropic growth of the nanofibers, and the structural transformation on heating is enabled by the weaker bonds between Co^{II} ions and water molecules. In this structure, the $\pi-\pi$ interactions between aromatic rings presumably significantly contribute to the structural stabilization.

It is worth noting that the lengths of the nanofibers can be easily tuned by simply controlling the concentrations of cobalt nitrate and sodium benzoate, while the widths of the nanofibers remain essentially unchanged. By decreasing the precursor salt concentrations, extremely long nanofibers of layered cobalt hydroxide up to several hundred micrometers can be formed. For instance, decreasing the concentration of both salts down to $^1/_4$ of the value used to prepare the material shown in Figures 1–3 yielded nanofibers with a length of about 220 μm (Figure 5a,c), with aspect ratios higher than 2000. This can be explained by the decreased number of nuclei due to the low reactant concentration, resulting in the higher probability of crystal collisions giving elongation of the nanofibers. Conversely, shorter nanofibers can be obtained by increasing the salt concentrations. For example, doubling the concentrations of the two starting materials used to prepare the material shown in Figures 1–3 produced shorter nanofibers of about 2 μm, as shown in Figure 5b,d.

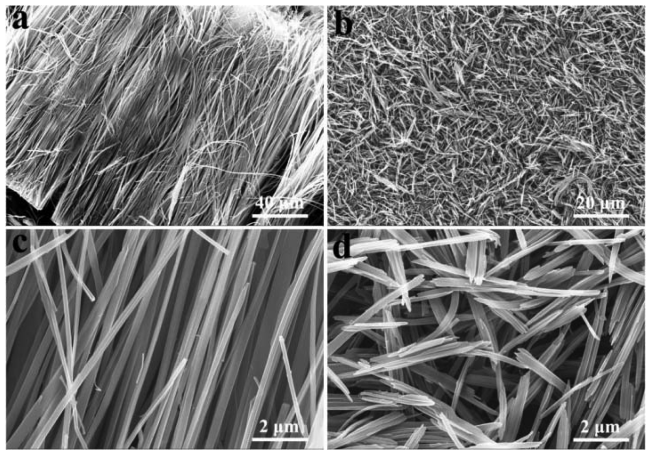

Figure 5. SEM images of the $Co(OH)(C_6H_5COO)\cdot H_2O$ nanofibers of different length obtained with (a, c) $^1/_4$ and (b, d) double the concentration of starting materials used to prepare the material shown in Figures 1–3.

CONCLUSIONS

In summary, high-quality, single-cryatalline organic–inorganic layered cobalt hydroxide nanofibers intercalated with benzoate anions have been controllably synthesized by a simple, green, and economical method. The prepared nanofibers are of high quality in terms of morphology, size, uniformity, crystallinity, and purity, and have been well-characterized by SEM/TEM/HRTEM/EDX/XRD/XPS/EA/FTIR/TGA/UV–vis. The results offer the first significant insights into the crystal structure of 1D layered cobalt hydroxide and demonstrate that the strong bridging coordination between metal layer and interlayer anions is the driving force for the formation of 1D nanostructure. We have also shown that the nanofibers exhibit a reversible transformation of the coordination geometry of the Co^{II} ions between octahedral and pseudotetrahedral, which involves the loss and reuptake of unusual weakly coordinated water molecules without loss of crystallinity. The resulting

dx.doi.org/10.1021/ic501812n | Inorg. Chem. 2014, 53, 12841–12847

properties of the nanofibers suggest that they could be used as building blocks for nanodevices in the fields of catalysis, gas storage or separation, magnetism, and sensors. Preliminary experimental results show that this method can also be used for the synthesis of other organic−inorganic layered metal hydroxide systems such as Zn-based, Ni-based, and Cu-based 1-D nanostructures, and these well-defined organic−inorganic may act as potential precursors to interesting oxide or sulfide nanostructures. Such research is ongoing in our laboratory.

■ ASSOCIATED CONTENT

Supporting Information

Co 2p XPS spectrum of $Co(OH)(C_6H_5COO)\cdot H_2O$ nanofibers; TGA curve of the rehydrated $Co(OH)(C_6H_5COO)\cdot H_2O$ nanofibers under N_2 gas flow; X-ray diffraction patterns of $Co(OH)(C_6H_5COO)\cdot H_2O$ nanofibers after treatment under different conditions; EDX spectrum, TGA curve, XRD spectra, UV−vis spectra, FTIR spectra of the green α-$Co(OH)_2$ nanoplates. This material is available free of charge via the Internet at http://pubs.acs.org.

■ AUTHOR INFORMATION

Corresponding Author

*E-mail: wangliany@mail.buct.edu.cn.

Author Contributions

The manuscript was written through contributions of all authors. All authors have given approval to the final version of the manuscript.

Notes

The authors declare no competing financial interest.

■ ACKNOWLEDGMENTS

This work was supported by the National Natural Science Foundation of China, Beijing Natural Science Foundation (2122048), and the Changjiang Scholars and Innovative Research Team in University (IRT1205).

■ REFERENCES

(1) (a) Xia, Y.; Yang, P.; Sun, Y.; Wu, Y.; Mayers, B.; Gates, B.; Yin, Y.; Kim, F.; Yan, H. *Adv. Mater.* **2003**, *15*, 353−389. (b) Yu, S.-H.; Liu, B.; Mo, M.-S.; Huang, J.-H.; Liu, X.-M.; Qian, Y.-T. *Adv. Funct. Mater.* **2003**, *13*, 639−647. (c) Ju, S.; Facchetti, A.; Xuan, Y.; Liu, J.; Ishikawa, F.; Ye, P.; Zhou, C.; Marks, T. J.; Janes, D. B. *Nat. Nanotechnol.* **2007**, *2*, 378−384. (d) Liu, B.; Chen, H. M.; Liu, C.; Andrews, S. C.; Hahn, C.; Yang, P. *J. Am. Chem. Soc.* **2013**, *135*, 9995−9998. (e) Kargar, A.; Jing, Y.; Kim, S. J.; Riley, C. T.; Pan, X.; Wang, D. *ACS Nano* **2003**, *7*, 11112−11120. (f) Kim, A.; Won, Y.; Woo, K.; Kim, C.-H.; Moon, J. *ACS Nano* **2003**, *7*, 1081−1091. (g) Li, P.; Liao, Q.; Yang, S.; Bai, X.; Huang, Y.; Yan, X.; Zhang, Z.; Liu, S.; Lin, P.; Kang, Z.; Zhang, Y. *Nano Lett.* **2014**, *14*, 480−485.

(2) (a) Hou, S.; Harrell, C. C.; Trofin, L.; Kohli, P.; Martin, C. R. *J. Am. Chem. Soc.* **2004**, *126*, 5674−5675. (b) Singh, R.; Pantarotto, D.; McCarthy, D.; Chaloin, O.; Hoebeke, J.; Partidos, C. D.; Briand, J.-P.; Prato, M.; Bianco, A.; Kostarelos, K. *J. Am. Chem. Soc.* **2005**, *127*, 4388−4396.

(3) (a) Pan, Z. W.; Dai, Z. R.; Wang, Z. L. *Science* **2001**, *291*, 1947−1949. (b) Mo, M.; Zeng, J.; Liu, X.; Yu, W.; Zhang, S.; Qian, Y. *Adv. Mater.* **2002**, *14*, 1658−1662. (c) Wang, Z. L. *Adv. Mater.* **2003**, *15*, 432−436. (d) Fang, X.; Bando, Y.; Liao, M.; Gautam, U. K.; Zhi, C.; Dierre, B.; Liu, B.; Zhai, T.; Sekiguchi, T.; Koide, Y.; Golberg, D. *Adv. Mater.* **2009**, *21*, 2034−2039.

(4) (a) Urban, J. J.; Yun, W. S.; Gu, Q.; Park, H. *J. Am. Chem. Soc.* **2002**, *124*, 1186−1187. (b) Cheng, B.; Russell, J. M.; Shi, W.; Zhang, L.; Samulski, E. T. *J. Am. Chem. Soc.* **2004**, *126*, 5972−5973. (c) Zhang, Z.; Rondinone, A. J.; Ma, J.-X.; Shen, J.; Dai, S. *Adv. Mater.* **2005**, *17*, 1415−1419. (d) Liang, Y.; Schwab, M. G.; Zhi, L.; Mugnaioli, E.; Kolb, U.; Feng, X.; Müllen, K. *J. Am. Chem. Soc.* **2010**, *132*, 15030−15037. (e) Zhang, J.; Jin, S.; Fry, H. C.; Peng, S.; Shevchenko, E.; Wiederrecht, G. P.; Rajh, T. *J. Am. Chem. Soc.* **2011**, *133*, 15324−15327.

(5) (a) Cheetham, A. K.; Rao, C. N. R.; Feller, R. K. *Chem. Commun.* **2006**, 4780−4795. (b) Zhang, X.; Chen, Z.-K.; Loh, K. P. *J. Am. Chem. Soc.* **2009**, *131*, 7210−7211. (c) Yuan, J.; Xu, Y.; Müller, A. H. E. *Chem. Soc. Rev.* **2011**, *40*, 640−655. (d) Ren, S.; Chang, L.-Y.; Lim, S.-K.; Zhao, J.; Smith, M.; Zhao, N.; Bulovirć, V.; Bawendi, M.; Gradečak, S. *Nano Lett.* **2011**, *11*, 3998−4002. (e) Gao, Q.; Wang, S.; Fang, H.; Weng, J.; Zhang, Y.; Mao, J.; Tang, Y. *J. Mater. Chem.* **2012**, *22*, 4709−4715. (f) Yang, L.; Wang, S.; Mao, J.; Deng, J.; Gao, Q.; Tang, Y.; Schmidt, O. G. *Adv. Mater.* **2013**, *25*, 1180−1184.

(6) (a) Gao, Q.; Zhang, C.; Wang, S.; Shen, W.; Zhang, Y.; Xu, H.; Tang, Y. *Chem. Commun.* **2010**, *46*, 6494−6496. (b) Wang, S.; Gao, Q.; Zhang, Y.; Gao, J.; Sun, X.; Tang, Y. *Chem.—Eur. J.* **2011**, *17*, 1465−1472. (c) Gao, Q.; Wang, S.; Tang, Y.; Giordano, C. *Chem. Commun.* **2012**, *48*, 260−262. (d) Zhuo, S.; Xu, Y.; Zhao, W.; Zhang, J.; Zhang, B. *Angew. Chem.* **2013**, *125*, 8764−8768.

(7) (a) Ma, R.; Liu, Z.; Takada, K.; Iyi, N.; Bando, Y.; Sasaki, T. *J. Am. Chem. Soc.* **2007**, *129*, 5257−5263. (b) Zhao, M.-Q.; Zhang, Q.; Zhang, W.; Huang, J.-Q.; Zhang, Y.; Su, D. S.; Wei, F. *J. Am. Chem. Soc.* **2010**, *132*, 14739−14741. (c) Shao, M.; Ning, F.; Zhao, J.; Wei, M.; Evans, D. G.; Duan, X. *J. Am. Chem. Soc.* **2012**, *134*, 1071−1077.

(8) (a) Poul, L.; Jouini, N.; Fiévet, F. *Chem. Mater.* **2000**, *12*, 3123−3132. (b) Liu, Z.; Ma, R.; Osada, M.; Takada, K.; Sasaki, T. *J. Am. Chem. Soc.* **2005**, *127*, 13869−13874. (c) Demessence, A.; Rogez, G.; Rabu, P. *Chem. Mater.* **2006**, *18*, 3005−3015. (d) Song, R.-Q.; Xu, A.-W.; Deng, B.; Li, Q.; Chen, G.-Y. *Adv. Funct. Mater.* **2007**, *17*, 296−306. (e) Ida, S.; Shiga, D.; Koinuma, M.; Matsumoto, Y. *J. Am. Chem. Soc.* **2008**, *130*, 14038−14039. (f) Wang, P.; Bai, B.; Hu, S.; Zhuang, J.; Wang, X. *J. Am. Chem. Soc.* **2009**, *131*, 16953−16960. (g) Wang, Y.; Zhang, H. J.; Lu, L.; Stubbs, L. P.; Wong, C. C.; Lin, J. *ACS Nano* **2010**, *4*, 4753−4761. (h) Xiong, S.; Chen, J. S.; Lou, X. W.; Zeng, H. C. *Adv. Funct. Mater.* **2012**, *22*, 861−871. (i) Gao, M.; Sheng, W.; Zhuang, Z.; Fang, Q.; Gu, S.; Jiang, J.; Yan, Y. *J. Am. Chem. Soc.* **2014**, *136*, 7077−7084.

(9) (a) Rujiwatra, A.; Kepert, C. J.; Rosseinsky, M. J. *Chem. Commun.* **1999**, 2307−2308. (b) Kurmoo, M. *J. Mater. Chem.* **1999**, *9*, 2595−2598. (c) Kurmoo, M. *Chem. Mater.* **1999**, *11*, 3370−3378. (d) Huang, Z.-L.; Drillon, M.; Masciocchi, N.; Sironi, A.; Zhao, J.-T.; Rabu, P.; Panissod, P. *Chem. Mater.* **2000**, *12*, 2805−2812. (e) Rujiwatra, A.; Kepert, C. J.; Claridge, J. B.; Rosseinsky, M. J.; Kumagai, H.; Kurmoo, M. *J. Am. Chem. Soc.* **2001**, *123*, 10584−10594. (f) Kurmoo, M.; Kumagai, H.; Hughes, S. M.; Kepert, C. J. *Inorg. Chem.* **2003**, *42*, 6709−6722. (g) Shimizu, H.; Okubo, M.; Nakamoto, A.; Enomoto, M.; Kojima, N. *Inorg. Chem.* **2006**, *45*, 10240−10247. (h) Delahaye, É.; Eyele-Mezui, S.; Bardeau, J.-F.; Leuvrey, C.; Mager, L.; Rabu, P.; Rogez, G. *J. Mater. Chem.* **2009**, *19*, 6106−6115. (i) Demessence, A.; Yassar, A.; Rogez, G.; Miozzo, L.; Brion, S. D.; Rabu, P. *J. Mater. Chem.* **2010**, *20*, 9401−9414. (j) Rogez, G.; Massobrio, C.; Rabu, P.; Drillon, M. *Chem. Soc. Rev.* **2011**, *40*, 1031−1058.

(10) (a) Hu, Z.-A.; Xie, Y.-L.; Wang, Y.-X.; Xie, L.-J.; Fu, G.-R.; Jin, X.-Q.; Zhang, Z.-Y.; Yang, Y.-Y.; Wu, H.-Y. *J. Phys. Chem. C* **2009**, *113*, 12502−12508. (b) Lee, J. H.; Du, Y.; O'Hare, D. *Chem. Mater.* **2009**, *21*, 963−968. (c) Liu, X.; Ma, R.; Bando, Y.; Sasaki, T. *Adv. Mater.* **2012**, *24*, 2148−2153. (d) Wang, L.; Dong, Z. H.; Wang, Z. G.; Zhang, F. X.; Jin, J. *Adv. Funct. Mater.* **2013**, *23*, 2758−2764.

(11) (a) Liu, X.; Ma, R.; Bando, Y.; Sasaki, T. *Angew. Chem., Int. Ed.* **2010**, *49*, 8253−8256. (b) Du, Y.; O'Hare, D. *Inorg. Chem.* **2008**, *47*, 11839−11846. (c) Liu, J.; Zhou, Y.; Liu, C.; Wang, J.; Pan, Y.; Xue, D. *CrystEngComm* **2012**, *14*, 2669−2674.

(12) Kooli, F.; Chisem, I. C.; Vucelic, M.; Jones, W. *Chem. Mater.* **1996**, *8*, 1969−1977.

(13) (a) Lebedev, O. I.; Millange, F.; Serre, C.; Tendeloo, G. V.; Férey, G. *Chem. Mater.* **2005**, *17*, 6525−6527. (b) Xiao, B.; Byrne, P. J.; Wheatley, P. S.; Wragg, D. S.; Zhao, X.; Fletcher, A. J.; Thomas, K.

M.; Peters, L.; Evans, J. S. O.; Warren, J. E.; Zhou, W.; Morris, R. E. *Nat. Chem.* **2009**, *1*, 289−294.
(14) (a) Xu, R.; Zeng, H. C. *Chem. Mater.* **2003**, *15*, 2040−2048. (b) Yang, J.; Liu, H.; Martens, W. N.; Frost, R. L. *J. Phys. Chem. C* **2010**, *114*, 111−119.
(15) Gavrilenko, K. S.; Punin, S. V.; Cador, O.; Golhen, S.; Ouahab, L.; Pavlishchuk, V. V. *J. Am. Chem. Soc.* **2005**, *127*, 12246−12253.
(16) (a) Inoue, S.; Fujihara, S. *Langmuir* **2010**, *26*, 15938−15944. (b) Inoue, S.; Fujihara, S. *Inorg. Chem.* **2011**, *50*, 3605−3612.
(17) (a) Deacon, G. B.; Philips, R. J. *Coord. Chem. Rev.* **1980**, *33*, 227−250. (b) Pinna, N.; Garnweitner, G.; Beato, P.; Niederberger, M.; Antonietti, M. *Small* **2005**, *1*, 112−121. (c) Wu, N.; Fu, L.; Su, M.; Aslam, M.; Wong, K. C.; Dravid, V. P. *Nano Lett.* **2004**, *4*, 383−286.
(18) Salah, M. B.; Vilminot, S.; André, G.; Richard-Plouet, M.; Mhiri, T.; Takagi, S.; Kurmoo, M. *J. Am. Chem. Soc.* **2006**, *128*, 7972−7981.
(19) (a) Weekhuysen, B. M.; Baetens, D.; Schoonheydt, R. A. *Angew. Chem., Int. Ed.* **2000**, *39*, 3419−3422. (b) Grandjean, D.; Beale, A. M.; Petukhov, A. V.; Weckhuysen, B. M. *J. Am. Chem. Soc.* **2005**, *127*, 14454−14465.
(20) Wang, L.; Lu, S.; Zhou, Y.; Guo, X.; Lu, Y.; He, J.; Evans, D. G. *Chem. Commun.* **2011**, *47*, 11002−11004.
(21) (a) Kitagawa, S.; Uemura, K. *Chem. Soc. Rev.* **2005**, *34*, 109−119. (b) Allan, P. K.; Xiao, B.; Teat, S. J.; Knight, J. W.; Morris, R. E. *J. Am. Chem. Soc.* **2010**, *132*, 3605−3611.
(22) (a) Chen, C.-L.; Goforth, A. M.; Smith, M. D.; Su, C.-Y.; zur Loye, H.-C. *Angew. Chem., Int. Ed.* **2005**, *44*, 6673−6677. (b) Takaoka, K.; Kawano, M.; Tominaga, M.; Fujita, M. *Angew. Chem., Int. Ed.* **2005**, *44*, 2151−2154. (c) Ouellette, W.; Prosvirin, A. V.; Whitenack, K.; Dunbar, K. R.; Zubieta, J. *Angew. Chem., Int. Ed.* **2009**, *48*, 2140−2143.
(23) Ma, R.; Liu, Z.; Takada, K.; Fukuda, K.; Ebina, Y.; Bando, Y.; Sasaki, T. *Inorg. Chem.* **2006**, *45*, 3964−3969.
(24) Laget, V.; Hornick, C.; Rabu, P.; Drillon, M.; Turek, P.; Ziessel, R. *Adv. Mater.* **1998**, *10*, 1024−1028.
(25) (a) Yang, J.; Sasaki, T. *Cryst. Growth Des.* **2010**, *10*, 1233−1236. (b) Wang, M.; Zeng, L.; Chen, Q. *Dalton Trans.* **2011**, *40*, 597−601.